Experimental and theoretical study of polarization in commercially available photonic crystal fibers

Rakhi Bhattacharya[1] · M. S. Mani Rajan[2] · A. Sharafali[3] · N. Ayyanar[4] · Hassan Pakarzadeh[5]

Abstract

In the present article experimentally we have measured optical polarization and birefringence in commercially available endlessly single mode photonic crystal fiber (PCF) named ESM-12B. We have applied the twist into the PCF using mechanical rotator in the experimental setup. The twist angle varied from 0° to 1440° with the interval of 360° rotation. Polarization and birefringence calculated for each twist angle using Polarimetry technique. It is observed from the experimental results that polarization and birefringence can be controlled by applying appropriate twist angle. Theoretical simulation is performed for optimization of the twist angle and calculation of dispersion for each twist angle with respect to wavelength from 0.6 μm to 1.8 μm. It is realized that initial value of dispersion for left rotation is less than -250 ps/nm/km but for right rotation initial value is less than -400 ps/nm/km. Application of the present work leads to use the PCF ESM-12B as polarization rotator and optical sensors.

Keywords Birefringence · Photonic crystal fibers · Polarimetry · Dispersion

1 Introduction

Optical fibres are used in a wide range of applications including telecommunication, medical, defense, industrial and commercial. In order to achieve high data rates in the area of telecomm particular, long haul, high data rate systems, and also used in the intrinsic fiber optic sensors. In order to fulfill the demand of latest technology commercially available

✉ M. S. Mani Rajan
  senthilmanirajanofc@gmail.com

1 Department of Physics, Koneru Lakshmaiah Educational Foundation, Aziz Nagar, Hyderabad, Telangana 500075, India

2 Department of Physics, University College of Engineering, Anna University, Ramanathapuram Campus , Ramanathapuram, Tamilnadu 623513, India

3 Department of Physics, Pondicherry University, Puducherry, India

4 Department of ECE, Thiagarajar College of Engineering, Madurai, Tamilnadu, India

5 Department of Physics, Shiraz University of Technology, Shiraz, Iran

endlessly single mode PCF particularly ESM-12B have come in picture which has the unique flexible features like controllable dispersion, non-linearity and loss with a property of endlessly single mode (Upadhyay et al. 2021a, 2021b, 2021c). When optical wavelength interacts with PCFs, the three physical parameters of light like polarization, amplitude and phase are used to carry information. Despite the benefits of fibre use, we must consider the negative impacts that exist in real non-ideal optical fibre. The existence of inherent and induced birefringence is critical in telecommunications (Singh et al. 2022) and sensing applications (Almawgani et al. 2022). The existence of birefringence might result in an unfavorable polarization shift.

Changes in the principal axis angle and phase retardance of the optical medium as a result of differences in the externally applied stress define birefringence effects. In other words, birefringence effects are caused by a feature of some optical media called "optical activity," which causes right-circularly polarized light to go through the medium at a different speed than left-circularly polarized light. The applications of birefringence effect are Strain-sensing systems, wave plates, glucose concentration monitoring devices, and etc. As a result, there are numerous proposals for determining the linear (Ulrich and Simon 1979; Rashleigh 1983) or circular (Kapron et al. 1972; Papp and Harms 1975) birefringence features of optical media. About two decades ago pioneering studies, establish precise relationship between the kind of perturbation acting on the fiber and the properties of the induced birefringence (Ulrich and Simon 1979; Rashleigh 1983; Kapron et al. 1972; Papp and Harms 1975). Twist has a close relationship with the linear birefringence that exists in any genuine fibre (Kapron et al. 1972; Papp and Harms 1975) as a result of deviations from a circular core form or owing to internal tension. Depending on the relative magnitudes of the twist rate X and the linear birefringence, three typical circumstances can be recognized. Linear birefringence is the dominating effect in the case of weak twist, and the twist rotates its principal axes. In terms of these axes, polarization evolves almost identically to how it would in a non-twisted fibre. As a result, the polarization gets twisted with the fibres.

Being able to characterize the birefringence of fibre structures (loops, helical coils) is crucial since birefringence has a substantial impact on many applications employing fibre. This test can be carried out utilizing a monochromatic input signal with known polarization and a polarimeter setup to measure the output signal. If the sample's birefringence matrix is known, both polarization states can be easily connected using matrix mathematics. As a result, validation of the birefringence matrix utilized to describe the birefringence properties of the fibre structure is a crucial aspect of this characterization procedure. In general, fibre architectures have two basic deformations: bend and twist; in this paper, we investigate the birefringence of twisted PCF.

The polarization ellipse of the output signal spins as the twist rises in an anisotropic medium. Twist generated birefringence, as Ulrich and Simon (Ulrich and Simon 1979) pointed out, is dependent on the intrinsic birefringence of any fibre. They propose that at medium twist, the shear strain in the twisted fibre generates circular birefringence, which is changed into elliptical birefringence when paired with the fiber's intrinsic linear birefringence.

An experimental examination of the polarization changes has observed when twist is applied to a commercially available continuously single mode (ESM-12B, 87 cm length) fibre with no intended birefringence. Rather than looking at the evolution of the state of polarization (SOP) along the fibre (Collett 1993; Tang and Kwok 2001; Shurcliff 1962; Kliger et al. 1990) on the Poincare sphere, we also looking for at the evolution of output Stokes parameters with torsion ranging from 0° to 1440°. It has been assumed that twisting

a fiber induces circular birefringence. Twist-induced alterations have been investigated by perturbation for an isotropic PCF. It has been demonstrated that the plane of polarization spins in the direction of twisted light path. Because the modification of the polarization state of transmitted light is the most common manifestation of birefringence phenomena, a brief recapitulation of polarization states and its illustrative is offered.

2 Theoretical modeling and design analysis of the PCF:

To undertake a theoretical analysis of twisted PCF, we assumed that the original birefringence is not changed, but that the geometric change. The PCF in this situation can be a sequence of equal birefringent plates with rotational birefringence axes. The birefringence axis of each differential plate that is rotated at the same angle as the previous plate is depicted in Fig. 1.

Further to continue the theoretical investigation we have implicit that for short endlessly single mode PCF sample the waveguide structure is uniform and they can be described as homogeneous retarders (elliptical retarders). Therefore, using the 3×3 Mueller matrix $M_e(\delta, \sigma)$ (Tsao 1992)

$$M_e = \begin{pmatrix} 1 - 2\cos^2 \sigma \sin^2 \left(\frac{\delta}{2}\right) & -\cos \sigma \sin \delta & -\sin 2\sigma \sin^2 (\delta/2) \\ \cos \sigma \sin \delta & \cos \delta & \sin \sigma \cos \delta \\ -\sin 2\sigma \sin^2 (\delta/2) & -\sin \sigma \sin \delta & 1 - 2\sin^2 \sigma \sin^2 (\delta/2) \end{pmatrix} \tag{1}$$

$$\sigma = \pi/2 - 2\varepsilon \tag{2}$$

$\varepsilon =$ Ellipticity angle; $\delta =$ Phase retardation between elliptical polarization eigen modes.

$$\delta^2 = (\delta_l^2) + (\delta_c^2) \tag{3}$$

where δ_l is linear shift and δ_c is circular shift, each transverse section is rotated with respect to the previous one an angle given by τ_l (angle of rotation per unit length of fiber). This means that two neighbouring differential cross sections at a distance dz rotate through a relative angle $d\omega = \tau_l dz$. For a fiber's length L the total torsion angle is $\tau = \omega L$. The retardation between elliptical polarization modes is depicted in Fig. 2. After mathematical analysis it is demonstrated that the new matrix (M_{GR}) (Tentori et al. 2009a; Chen et al. 2015) including the contribution of the geometric rotation of the birefringence axes is given by,

$$M_{GR} = R(b\tau)M_e(\delta, \sigma) \tag{4}$$

Fig. 1 Rotation of birefringence axes of twisted PCF
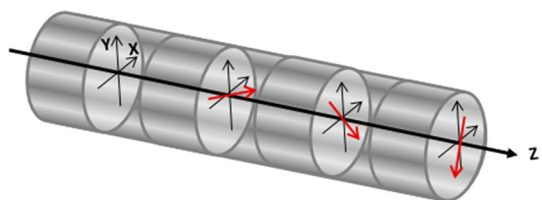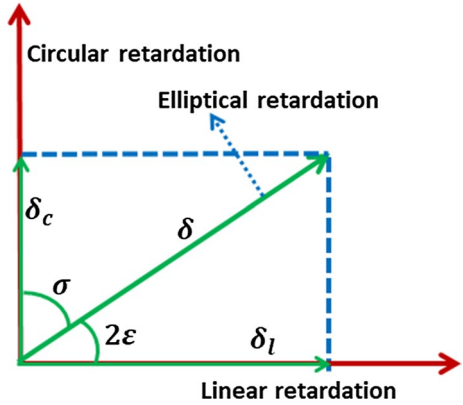
Fig. 2 Representation of linear, circular and elliptical retardation

Which is the product of two matrices: $M_e(\delta, \sigma)$ that describes the anisotropy of the medium given by the residual birefringence of the straight fiber and a rotation matrix that includes the total angle of torsion. The rotation matrix $R(b\tau)$ includes the total angle of rotation (Tsao 1992),

$$R(b\tau) = \begin{pmatrix} \cos 2b\tau & -\sin 2b\tau & 0 \\ \sin 2b\tau & \cos 2b\tau & 0 \\ 0 & 0 & 1 \end{pmatrix} \text{with } b = 1 \qquad (5)$$

Twist $|\tau| \simeq |\beta|$

In this case we assume that the total induced elliptical retardance δ_τ varies linearly with τ, $\alpha = g\tau$, $\delta_\tau = \delta_0 + c\tau$, where c is an unknown constant and δ_0 is the retardance value for $\tau = 0$, that is δ_0 represents the retardance value due to the fiber's residual birefringence. This value can be used of δ_τ in Eq. (1) to obtain the below equation (Tsao 1992),

$$M_\tau(\delta_{\tau,\sigma}) = \begin{pmatrix} 1 - 2\cos^2 \sigma \sin^2\left[\frac{\delta_\tau}{2}\right] & \cos \sigma \sin \delta_\tau & \sin 2\sigma \sin^2\left[\frac{\delta_\tau}{2}\right] \\ \cos \sigma \sin \delta_\tau & \cos \delta_\tau & \sin \sigma \sin \delta_\tau \\ = -\sin 2\sigma \sin^2\left[\frac{\delta_\tau}{2}\right] & -\sin \sigma \sin \delta_\tau & 1 - 2\sin^2 \sigma \sin^2\left[\frac{\delta_\tau}{2}\right] \end{pmatrix} \qquad (6)$$

If we have a linear polarization state S_{in} with azimuth angle ϕ given by,

$$S_{in}(\phi) = \begin{bmatrix} \cos(2\beta) \\ \sin(2\phi) \\ \phi 0 \end{bmatrix} \qquad (7)$$

The Stokes parameters S1 and S2 present a fixed azimuth shift of 180^0, therefore, we propose that the total matrix for twist induced birefringence is $S_{out} = M_T(\beta, \tau, \delta_\tau, \sigma, \theta) \sin_{in}(\phi)$. The output Stokes vector S_{out} can be found to be

$$S_{out} = \left\{ S1_{out}, S2_{out}, S3_{out} \right\} \qquad (8)$$

$$
\begin{aligned}
S1_{out} = & -\sin\left[2(b\tau - \theta + \beta)\right]\{\cos\sigma\sin\delta_\tau\cos 2(\phi - \theta) \\
& + \cos\delta_\tau\sin 2(\phi - \theta)\} + \cos 2(b\tau - \theta + \beta) \\
& + \{1 - 2\cos^2\sigma\sin^2[\delta_\tau/2]\cos 2(\phi - \theta) - \cos\sigma\sin\delta_\tau\sin 2(\phi - \theta)\}
\end{aligned}
\tag{9}
$$

$$
\begin{aligned}
S2_{out} = & \cos 2(b\tau - \beta + \theta)\{\cos\sigma\sin\delta_\tau\cos 2(\phi - \theta) + \cos\delta_\tau\sin 2(\phi - \theta)\} \\
& + \sin 2(b\tau - \theta + \beta) \\
& + \left\{1 - 2\cos^2\sigma\sin^2\left[\frac{\delta_\tau}{2}\right]\right\}\cos 2(\phi - \theta) - \cos\sigma\sin\delta_\tau\sin 2(\phi - \theta)\}
\end{aligned}
\tag{10}
$$

$$
S3_{out} = -\sin^2\left[\frac{\delta_\tau}{2}\right]\sin 2\sigma\cos 2(\phi - \theta) - \sin\delta_\tau\sin\sigma\sin 2(\phi - \theta)
\tag{11}
$$

3 Experimental setup

Figure 3 shows an experimental setup for measuring the input and output states of polarisation using the Stokes polarimetry approach (Wang and Oakberg 1999). A polarizer P1 is used to polarise the Gaussian beam from an unpolarized (5mW, 632.8 nm) He–Ne laser. After that, the linearly polarised light travels via a half-wave plate positioned on a rotation stage, allowing the polarisation direction of the input beam released into the PCF to be adjusted. After passing through the polarisation components, the beam is focused onto the cleaved end of the ESM-12B PCF, which is positioned using a three-axis stage, using a 0.4 NA 10 microscope objective lens OL1. Figure 4 shows the original picture of the scanning electron microscope (SEM) image of ESM 12B. The PCF is 87 cm long and is kept horizontal with one end fixed and the other end mounted with a mechanical rotator (MR) to generate twist.

At the output end another microscopic lens OL2 with 0.41 NA is used to collimate the beam. Quarter wave plate (QWP) with combination of polarizer P2 is placed at output end connected with CCD camera and computer to collect out beam for measuring Stokes parameters. Two cases are considered in the above setup; In the first case we have kept
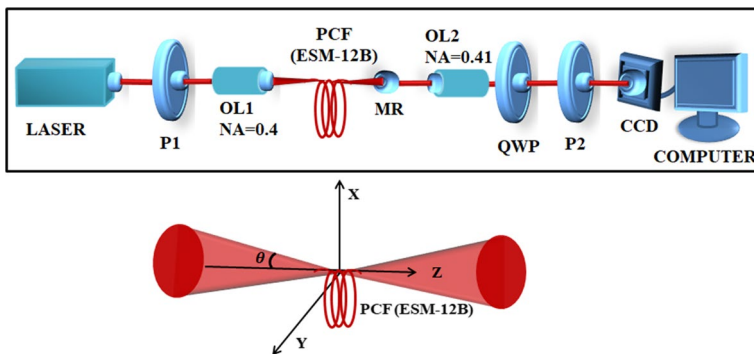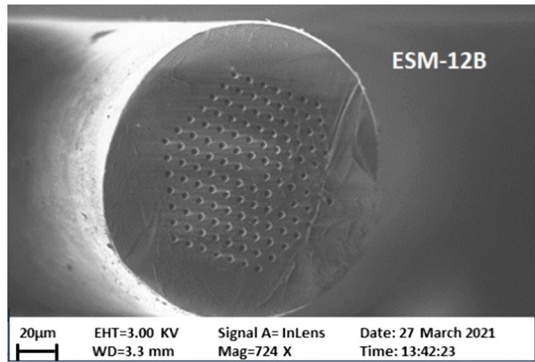

Fig. 3 Experimental setup used for the measurement of birefringence due to twist. P1, P2-polarizer; OL1, OL2-objective lenses; PCF- photonic crystal fiber; MR-mechanical rotator, CCD-camera

Fig. 4 SEM image of cross sectional view of endlessly single mode PCF ESM 12B

the input state of polarization constant and changed the twist rate for each measurement. To analyse the output state of polarization Stokes parameters are taken into account (Lo et al. 2004; Cameron and Cote 1997; Lo and Yu 2006). The Stokes parameters describe any polarisation condition of light in detail. Originally, the Stokes parameters were simply employed to define the optical field's measured intensity and polarisation state (Tentori et al. 2009b). In the second case we have changed the input state of polarization for each twist and performed the same measurements (Hameed et al. 2020).

4 Results and discussion

4.1 Experimental results

The birefringence matrix is a unitary transformation since it is the product of two unitary matrices. This behaviour may be validated by changing the azimuth angle of the input linear polarization state in the experimental setup. In our case input state of polarization is fixed, a linearly polarized horizontal beam is launched into the PCF with an objective lens. At the output end Stokes polarimetry setup is used to measure Stokes parameter, normalized Stokes parameter are calculated and shown in Fig. 5 for various twist angle. The measurement has performed for five different twist angles from $0°$ to 1440^0 with an interval of $360°$. Initially when no twist is applied i.e. twist angle is 0^0, the normalized Stokes parameters are depicted in Fig. 5B. An algorithm is developed to extract the normalized Stokes parameters from the experimentally measured data. Total intensity S0, horizontal and vertical components S1, diagonal and anti-diagonal components S2, right circularly polarized (RCP) and left circularly polarized (LCP) component S3 is calculated and plotted for each twist angle varied from 0^0 to 1440^0.Stokes measurements can be performed as follows,

$$S_0 = I\left(0^0, 0^0\right) + I\left(90^0, 0^0\right)$$

$$S_1 = I\left(0^0, 0^0\right) - I\left(90^0, 0^0\right)$$

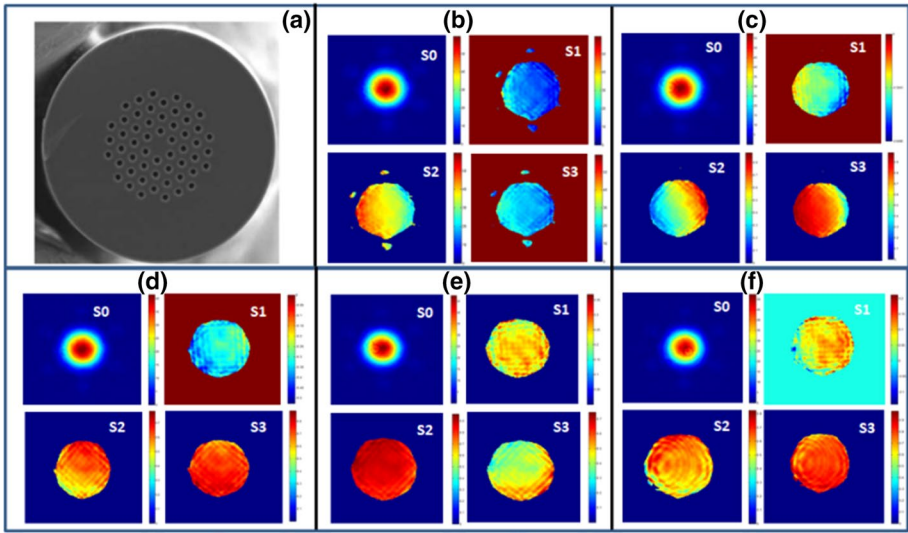$$S_2 = I\left(45^0, 0^0\right) - I\left(135^0, 0^0\right)$$

Fig. 5 Measured normalized Stokes parameter at twist angle **B** 0°, **C** 360°, **D** 720°, **E** 1080° and **F** 1440° of PCF at horizontal input polarization

$$S_3 = I(45^0, 90^0) - I(135^0, 90^0)$$

$I(\theta, \delta)$ intensity of the light variation in the direction which makes an angle θ with the x- axis direction after the phase retardation δ.

Ellipticity $\chi = \frac{1}{2}\sin^{-1}(S_3/S_0)$ and ellipse orientation $\alpha = \frac{1}{2}\tan^{-1}(S_2/S_1)$ are calculated by measured data and ellipse orientations are shown in Fig. 6. From Fig. 6a it is clear that direction of polarization ellipse and ellipticity changes clockwise as the twist angle is increased. Input state of polarization is fixed for the evolution of the output state of polarization measured for the endlessly single mode PCF (ESM-12B). Orientation of polarization ellipse without any twist angle for various input state of polarization is shown in Fig. 7 for ESM-12B PCF. It is observed from Fig. 7 that orientation of polarization ellipse and ellipticity changes with different state of input polarization without introducing any external twist. For right and left circularly polarized beams the measured ellipticity is more.
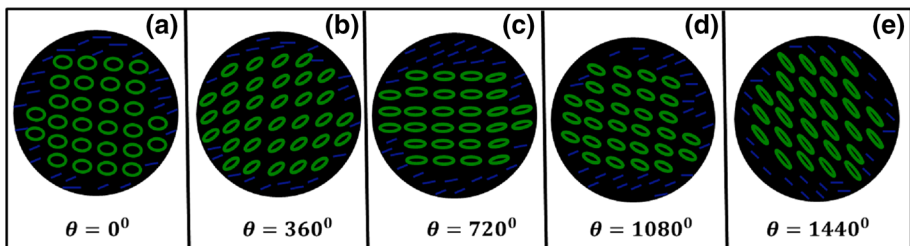

Fig. 6 Ellipse orientation of ESM-12B PCF at twist angle (a) 0°, (b) 360°, (c) 720°, (d) 1080° and **e** 1440° for horizontal input polarization
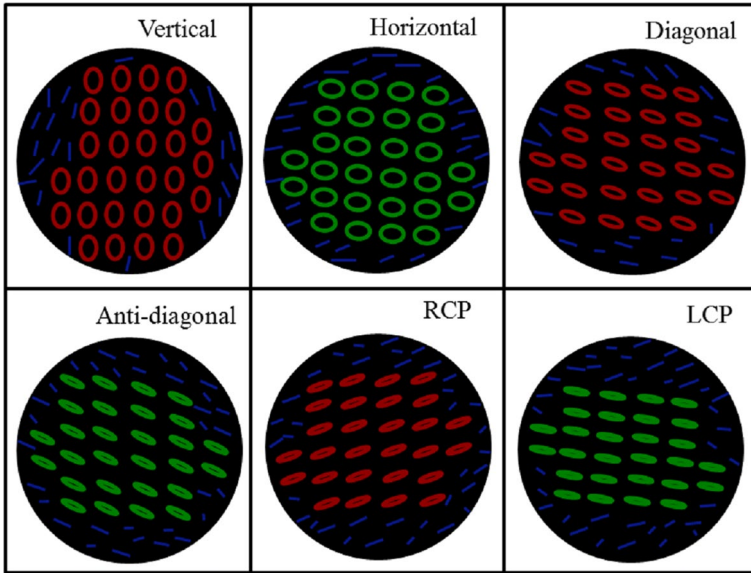
Fig. 7 Ellipse orientation of ESM-12B at twist angle $0°$ for different input state of polarization

When this fiber is twisted at a low twist rate, the components S1 and S2 of the Stokes vector S_{out} are modified.

4.2 Simulation results

Theoretical simulation has been performed for various twist angles of PCF i.e. 0^0 to 1440^0 for horizontal and vertical polarization for optimization of the twist angle for controlling polarization. Using finite element method (FEM), the permanent twist can be applied at the cladding surface of the PCF. Followed by the experimental study, the circular polarization for proposed structure is induced right and left rotation and the pattern is simulated for different angle ($360°$, $720°$, 1080^0 and $1440°$). Initially for the case of untwisted PCF, the polarization in horizontal and vertical direction is plotted in Fig. 8b c and after applying
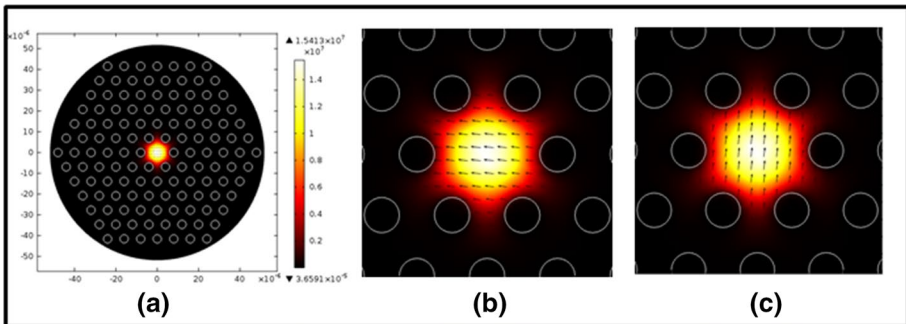

Fig. 8 Polarization inducement of untwisted PCF at $0°$, **a** Horizontal polarization, **b** Vertical polarization
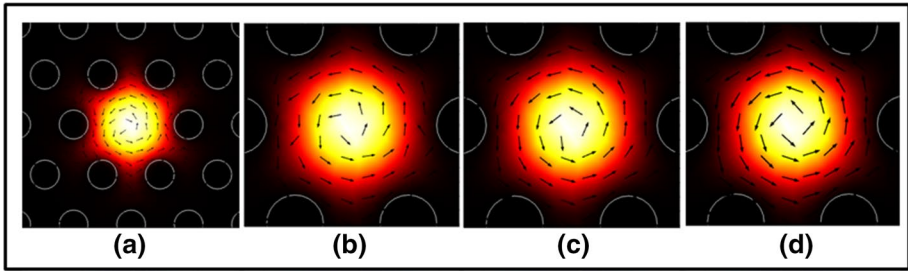
Fig. 9 Polarization inducement of twisted PCF for left rotation **a** 360°, **b** 720°, **c** 1080° and **d** 1440^{0}
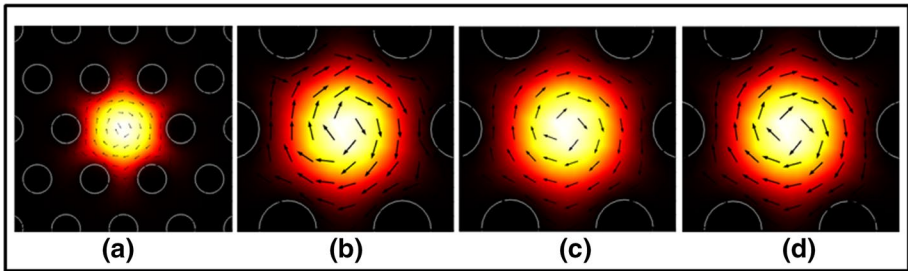
Fig. 10 Polarization inducement of twisted PCF for right rotation **a** 360°, **b** 720°, **c** 1080° and **d** 1440°

twist; the induced circular polarization for left and right rotation is given in Fig. 9a-d for different rotation angle and Fig. 10a-d respectively.

To analyze the impact of twist over dispersion for circular polarization, we have calculated waveguide (Bhattacharya 2018; Bhattacharya and Konar 2012; Mogilevtsev et al. 1998) for the case of left and right circularly polarized modes. As the polarization effects gives the circular symmetry (Prajapati 2021a, 2021b, 2021c; Prajapati and Viswanathan 2019; Pakarzadeh and Sharif 2019), the energy confinement gets maximum in the core region than the cladding section and hence the loss gets minimum which reflects negative dispersion characteristics and its tendency is moving upward while increasing the wavelength. Increase in the dispersion may cause of more number of twisting and increasing the squeezing effect on optical power distribution is more and it may decay from its maximum core penetration resulting for incremental dispersion characteristics. The wavelength is varied from 0.6 mμ to 1.8 mμ and the calculated dispersion is plotted in Fig. 11(a) and (b). It is exhibited that starting value of dispersion for left rotation is below -250 ps/nm/km but for right rotation it is below - 400 ps/nm/km. The outreach of waveguide dispersion performance is attained better for right rotation than the left rotation. For the maximum wavelength of 1.8 mμ, it reaches rotation, and squeezing effect on optical power distribution which may decay from its maximum core penetration. The wavelength is varied from 0.6 mμ to 1.8 mμ and the calculated dispersion is plotted in Fig. 11(a),(b). The effect of variation is merely uniform for left and right rotation but the value of dispersion is differed for both rotations, 48.4 ps/nm/km for left rotation and 27.4 ps/nm/km for right rotation. While matching with experimental curve characteristics, it has been done with merely similar behavior for both rotations.

Fig. 11 waveguide dispersion of twisted PCF for both **a** left rotation, **b** right rotation at different twisted angle
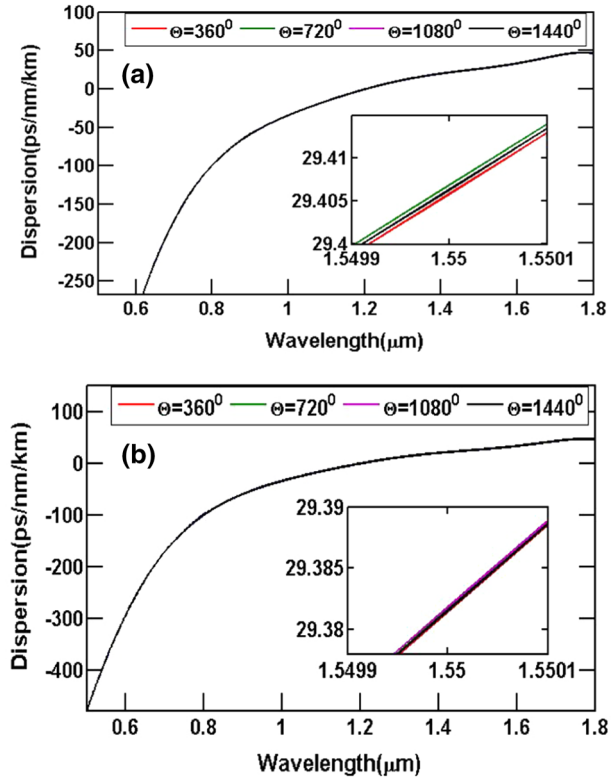
5 Conclusion

In the present article very first time investigation of commercially available twisted ESM-12B PCF is presented. The dynamic behavior of the polarization rotation is observed and birefringence calculation is performed. Theoretical simulation for polarization and dispersion calculation is procured with respect to wavelength from 0.6 μm to 1.8 μm at various twist angle. in this article. It is verified from experimental and theoretical simulation that state of polarization is varying with change in the PCF twist angle. Dispersion is calculated for both left and right circularly polarized mode and it is observed that the.

value of dispersion is differed for both rotations. It is realized that initial value of dispersion for left rotation is less than − 250 ps/nm/km but for right rotation initial value is less than -400 ps/nm/km. The present investigation of PCF can be exploited in applications of polarization rotator and optical sensors. Our investigation presents the significant highly dynamical nature of the evolution of the change in polarization with applied twist angle.

Data availability statement Data sharing is not applicable to this article as no new data were created or analyzed in this study. We do not use previously published data in our work.

Declarations

Conflicts of interest The authors declare that they have no known competing financial interests or personal relationships that could have appeared to influence the work reported in this paper.

References

Almawgani, A.H.M., Taya, S.A., Daher, M.G., Colak, I., Feng, Wu., Patel, Shobhit K.: Detection of glucose concentration using a surface plasmon resonance biosensor based on barium titanate layers and molybdenum disulphide sheets. Physica Scripta **97**(6), 065501 (2022)

Bhattacharya, R.: Generation of phase singular optical beams in microstructure optical fibers. Optics Communications **428**, 15–21 (2018)

Bhattacharya, R., Konar, S.: Dual-core photonic crystal fibers for dispersion compensation. J. Nanophotonics **6**(1), 063520 (2012)

Cameron, B.D., Cote, G.L.: Noninvasive glucose sensing utilizing a digital closed-loop polarimetric approach. IEEE Trans. Biomed. Eng. **44**(12), 1221–1227 (1997)

Chen, L., Zhang, W.G., Yan, T.Y., Wang, L., Sieg, J., Wang, B., Zhou, Q., Zhang, L.Y.: Photonic crystal fiber polarization rotator based on the topological Zeeman effect. Opt. Lett. **40**(15), 3448–3451 (2015)

Collett, E.: Polarized Light: Fundamentals and Applications. Marcel Dekkar. Inc, NY (1993)

Hameed, M.F.O., Esmail, M.S.M., Obayya, S.S.: Terahertz photonic crystal fiber polarization rotator. JOSA B **37**(10), 2865–2872 (2020)

Kapron, F., Borrelli, N., Keck, D.: Birefringence in dielectric optical waveguides. IEEE J. Quantum Electron. **8**(2), 222–225 (1972)

Kliger D.S., Lewis J.W., Randall C.E. 1990 Polarized Light in Optics and Spectroscopy Academic Press, San Diego.

Lo, Y.L., Yu, T.C.: A polarimetric glucose sensor using a liquid-crystal polarization modulator driven by a sinusoidal signal. Optics Communications **259**(1), 40–48 (2006)

Lo, Y.L., Lai, C.H., Lin, J.F., Hsu, P.F.: Simultaneous absolute measurements of principal angle and phase retardation with a new common-path heterodyne interferometer. Appl. Opt. **43**(10), 2013–2022 (2004)

Mogilevtsev, D., Birks, T.A., Russell, P.S.J.: Group-velocity dispersion in photonic crystal fibers. Opt. Lett. **23**(21), 1662–1664 (1998)

Pakarzadeh, H., Sharif, V.: Control of orbital angular momentum of light in optofluidic infiltrated circular photonic crystal fibers. Optics Communications **438**, 18–24 (2019)

Papp, A., Harms, H.: Polarization optics of index-gradient optical waveguide fibers. Appl. Opt. **14**(10), 2406–2411 (1975)

Prajapati, C.: Light refraction from a uniaxial crystal with arbitrary optic axis orientation using matrix representation. Optik **237**, 166656 (2021a)

Prajapati, C.: Study of electric field vector, angular momentum conservation and poynting vector of nonparaxial beams. J. Opt. **23**(2), 025604 (2021b)

Prajapati, C.: Numerical study of spin–orbit interaction of light in nonparaxial focusing of Gaussian beams. Optik **228**, 166199 (2021c)

Prajapati, C., Viswanathan, N.K.: Observation of diffractive-correction and spin-orbit interaction induced effects around the Brewster angle. J. Opt. **21**(8), 084002 (2019)

Rashleigh, S.: Origins and control of polarization effects in single-mode fibers. J. Lightwave Technol. **1**(2), 312–331 (1983)

Shurcliff, W.A.: Polarized Light: Production and Use Harvard U, p. 16. Press, Cambridge, Mass (1962)

Singh, S., Upadhyay, A., Sharma, D., Taya, S.A.: A comprehensive study of large negative dispersion and highly nonlinear perforated core PCF: theoretical insight. Phys. Scr. **97**(6), 065504 (2022)

Tang, S.T., Kwok, H.S.: 3× 3 Matrix for unitary optical systems. JOSA A **18**(9), 2138–2145 (2001)

Tentori, D., Ayala-Díaz, C., Ledezma-Sillas, E., Treviño-Martínez, F., García-Weidner, A.: Birefringence matrix for a twisted single-mode fiber: Geometrical contribution. Optics Communications **282**(5), 830–834 (2009b)

Tentori, D., Ayala-Díaz, C. and Treviño-Martínez, F., 2009a, December. Twist-induced birefringence in fibers and optical rotation. In Seventh Symposium Optics in Industry (Vol. 7499, p. 749910). International Society for Optics and Photonics.

Tsao, C.: Optical fibre waveguide analysis. Oxford University Press (1992)

Ulrich, R., Simon, A.: Polarization optics of twisted single-mode fibers. Appl. Opt. **18**(13), 2241–2251 (1979)

Upadhyay, A.S., Divya Sharma, S., Taya, S.A.: highly birefringent bend-insensitive porous core PCF for endlessly single-mode operation in THz regime: an analysis with core porosity. Appl. Nanosci. **11**(3), 1021–1030 (2021a)

Upadhyay, A., Singh, S., Sharma, D., Taya, S.A.: An ultra-high birefringent and nonlinear decahedron photonic crystal fiber employing molybdenum disulphide (MoS2): a numerical analysis. Mater. Sci. Eng., B **270**, 115236 (2021c)

Upadhyay, A. Shivam S. Divya Sharma, and Sofyan A. Taya., 2021b, Analysis of proposed PCF with square air hole for revolutionary high birefringence and nonlinearity, Photonics and Nanostructures-Fundamentals and Applications 43, 100896.

Wang, B., Oakberg, T.C.: A new instrument for measuring both the magnitude and angle of low level linear birefringence. Rev. Sci. Instrum. **70**(10), 3847–3854 (1999)